View metadata, citation and similar papers at core.ac.uk
brought to you by CORE
provided by PolyU Institutional Repository

Study of Stability Regions in Parallel Connected Boost Converters

Yuehui Huang and Chi K. Tse
Department of Electronic and Information Engineering
The Hong Kong Polytechnic University, Kowloon, Hong Kong
Email: yuehui.huang@polyu.edu.hk, encktse@polyu.edu.hk

***Abstract*— This paper describes the coexisting attractors of parallel connected boost switching converters under a master-slave current sharing scheme. We present the basins of attraction of desired and undesired attractors, which provide design information on the conditions for hot-swap operations. The system employs a typical proportional-integral (PI) controller for regulation. It is shown that the system will converge to different attractors for different initial conditions with the same control parameters. Simulation results are given to illustrate the phenomenon. This study is relevant to practical design. Specifically, we show that the stability regions obtained from linear methods (i.e., considering only local stability) can be over-optimistic as the global stability regions are found to be more restrictive in the parameter space.**

I. Introduction

Power supplies based on paralleling switching converters offer a number of advantages over a single, high-power, centralized power supply. They enjoy low component stresses, increased reliability, ease of maintenance and repair, improved thermal management, etc. [1], [2]. Paralleling of standardized converters is an approach used widely in distributed power systems for both front-end and load converters. Since current sharing has to be maintained among the paralleled converters, some form of control has to be used to equalize the individual currents in the converters. One widely used method for balancing currents is the *master-slave current sharing* method [3], [4].

The system under study in this paper is a parallel connected system of two boost converters. Under the master-slave scheme, one of the converters is the master and the other is the slave. Both of the converters are under peak-current-mode (PCM) control. The master consists of a typical proportional-integral (PI) control, to regulate the output voltage, and a comparator, to compare the feedback current with the reference current. The slave basically sets its current to equal that of the master via an active loop involving comparison of the currents of the two converters, as shown in Fig. 1. Previous studies of such systems have focused on pure proportional control, which is not normally used in practice [5]. The use of PI control introduces a low-pass characteristic to the feedback loop, thereby suppressing high-frequency components in the feedback signal. The resulting bifurcation and stability behavior is therefore different. In this paper we will consider practical PI control in our simulation study.

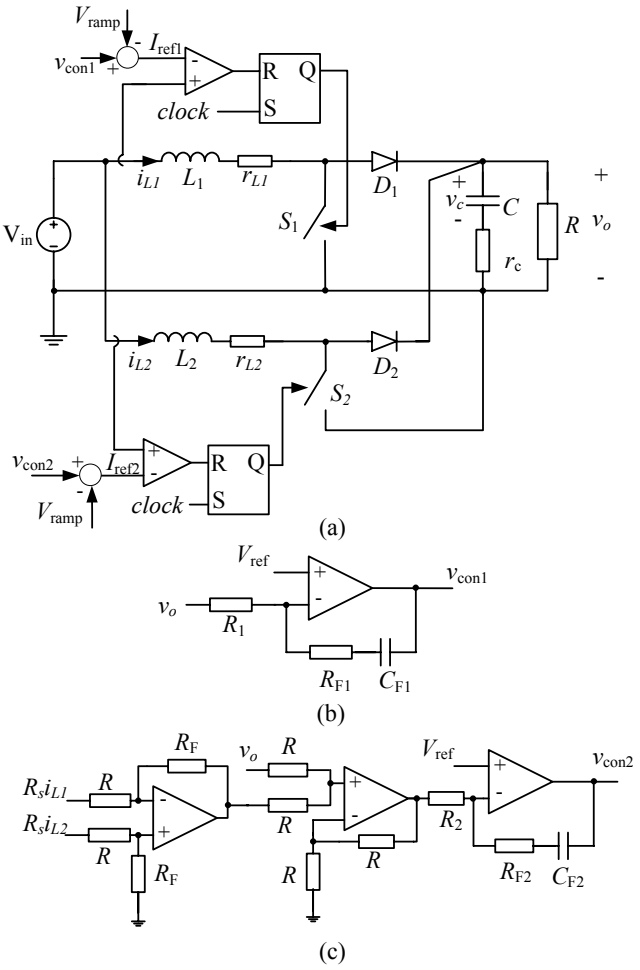

Fig. 1. Paralleled boost converters under master-slave current sharing.

Basically we find that for parallel connected boost converters, the desired operating orbit is not always reached from all initial conditions, even though the orbit has been found locally stable (e.g., from a linearized model). Depending on the initial state, the system may converge to different attractors, which can be a stable period-1 orbit, quasi-periodic orbit or chaotic orbit. In the paper, we examine two parallel connected boost converters with PCM control under master-slave current sharing. And it is easy to extend to N-paralleled converters. We show that different initial conditions may lead to different

1-4244-0449-5/06/$20.00 ©2006 IEEE

Authorized licensed use limited to: Hong Kong Polytechnic University. Downloaded on December 18, 2008 at 21:51 from IEEE Xplore. Restrictions apply.

steady states. Thus, linear stability analysis methods, which basically evaluate the convergence of the system trajectory to the desired steady state starting from a nearby point, can be misleading.

In this paper, we report the phenomenon, present specific basins of attraction for the different attractors, and derive the critical values of control parameters for which the system loses stability of its expected operation. We generally observe that stability boundaries obtained from equivalent linear methods are over-optimistic, in that the system is actually more prone to instability. Thus, reliable stability information can only be obtained with the basin of attractions duly taken into consideration.

II. System Description and Operation

Figure 1 (a) shows two boost converters connected in parallel. In this circuit, S_1 and S_2 are switches, which are under peak-current-mode (PCM) control. In the PCM, The switch is set to be on by the latch at the beginning of each cycle. Then if the feedback current reaches the reference current $I_{\rm ref}$, the switch will be turned off. The reference current is decided by the output of voltage regulator and the ramp compensation. The compensatory ramp signal is given by

$$V_{\rm ramp} = V_L + (V_U - V_L)\left(\frac{t}{T_s} \bmod 1\right) \tag{1}$$

where V_L and V_U are the lower and upper thresholds of the ramp, respectively, and T_s is the switching period. The role of ramp compensation is to stabilize the system when duty cycle exceeds 0.5 in peak current-mode-control.

The control signals $v_{\rm con1}$ and $v_{\rm con2}$ are derived from the voltage compensator, as shown in Figs. 1 (b) and (c). Here the compensator is a PI controller, e.g.,

$$\frac{V_{\rm con1}(s)}{E(s)} = -K_p\left(1 + \frac{1}{\tau_{F1}s}\right) \tag{2}$$

where $V_{\rm con1}(s)$ and $E(s)$ are the Laplace transforms of $v_{\rm con1}(t)$ and $e(t)$; $e(t)$ is the error between reference and output; K_p and τ_{F1} are the control parameters. With respect to the slave, extra current sharing signal is included. We can likewise write the equation.

We assume that the converter operates in continuous conduction mode (CCM) and diodes D_1 and D_2 are always in complementary state to S_1 and S_2. Consequently, the state equations of the converter stage of Fig. 1 are

$$\begin{cases} \dot{i}_{L1} = \frac{1}{L1}[V_{in} - r_{L1}i_{L1} - (1-q_1(t))v_o] \\ \dot{i}_{L2} = \frac{1}{L2}[V_{in} - r_{L2}i_{L2} - (1-q_2(t))v_o] \\ \dot{v}_c = \frac{1}{C}[(1-q_1(t))i_{L1} + (1-q_2(t))i_{L2} - \frac{v_o}{R}] \end{cases} \tag{3}$$

where v_o can be written as

$$\begin{aligned} v_o &= v_c + r_c i_c \\ &= v_c + r_c[(1-q_1(t))i_{L1} + (1-q_2(t))i_{L2} - \frac{v_o}{R}] \end{aligned} \tag{4}$$

and $q_1(t)$ and $q_2(t)$ are the switching function decided by the output of controllers. They are time varying functions given by

$$q_i(t) = \begin{cases} 1, \text{ if } S_i \text{ is on,} \\ 0, \text{ if } S_i \text{ is off.} \end{cases} \tag{5}$$

Depending upon the feedback circuit in Figs. 1(b) and (c), we have

$$\frac{dv_{\rm con1}}{dt} = -K_1\frac{dv_o}{dt} - \frac{K_1}{\tau_{F1}}v_o + \frac{K_1}{\tau_{F1}}V_{\rm ref} \tag{6}$$

$$\begin{aligned} \frac{dv_{\rm con2}}{dt} &= -K_2\frac{dv_o}{dt} - \frac{K_2}{\tau_{F2}}v_o + K_2K_i(\frac{di_{L1}}{dt} - \frac{di_{L2}}{dt}) \\ &+ \frac{K_2K_i}{\tau_{F2}}(i_{L1} - i_{L2}) + \frac{K_2}{\tau_{F2}}V_{\rm ref} \end{aligned} \tag{7}$$

where K_1 and K_2 are the proportional coefficients, τ_{F1} and τ_{F2} are the integral coefficients, K_i is the current sharing coefficient, and $V_{\rm ref}$ is the reference voltage (expected output voltage). In circuit terms, $K_1 = R_{F1}/R_1$, $\tau_{F1} = R_{F1}C_{F1}$, $K_2 = R_{F2}/R_2$, $\tau_{F2} = R_{F2}C_{F2}$, $K_i = R_F R_s/R$, where R_s is the current sensing resistance. Equations (6) and (7), together with (3), form the complete set of state equations of the system. It is a fifth order system.

III. Basins of Attraction

In this section, we begin our investigation of the basins of attraction of the operation orbits. Our simulations are based on the state equations derived in the foregoing section and hence are exact cycle-by-cycle simulations. We are primarily concerned with the system stability in relation to the initial condition X_0 ($X = [i_{L1}, i_{L2}, v_c]$ refers to the converter state variables), feedback parameters of the PI controller K_1, K_2, τ_{F1}, τ_{F2} and current sharing coefficient K_i. The circuit parameters and component values are listed in Table I.

TABLE I
Component Values Used in Simulations

Circuit Components	Values
Switching Period T_s	10 μs
Input Voltage $V_{\rm in}$	5 V
Reference Voltage $V_{\rm ref}$	10 V
Ramp Voltage V_L,V_U	0 V, 0.8 V
Inductance L_1, ESR r_{L1}	50 μH, 0.01 Ω
Inductance L_2, ESR r_{L2}	60 μH, 0.1 Ω
Capacitance C, ESR r_c	126 μF, 0 Ω
Load Resistance R	2 Ω
Current sensing Resistance R_s	0.01 Ω

Under the same controller but with different initial conditions, we find that the system will converge to stable period-1 orbit or unstable orbits as well as what we found in paralleled buck converters [6]. Again, there are more than one attractor in paralleled boost converters. The steady-state behavior of the system depends on where it starts [7]. The basins of attraction are therefore important.

In the following, we find the basin boundaries numerically in relation to initial point X_0, and determine how they are

Authorized licensed use limited to: Hong Kong Polytechnic University. Downloaded on December 18, 2008 at 21:51 from IEEE Xplore. Restrictions apply.

affected by the controller parameters K_1, K_2, τ_{F1} and τ_{F2}, as shown in Figs. 2, 3, 4 and 5. Figures 2 and 3 show the basins of attraction for different K_1 and K_2. We first get the boundary of stable and unstable operations in the i_{L1}–i_{L2} plane, and then extend it to a 3-D space by gathering boundaries for different v_{c0}. Figures 2 (a), (b), (c) and (d) are basins of attraction presented on the i_{L1}–i_{L2} plane for different initial v_{c0} with $K_1 = K_2 = 5$. The yellow region is the basin corresponding to the desired operating orbit (stable region), whereas the blue region is the basin corresponding to attractors other than the desired operating orbit (unstable region). Thus, if the system starts from the blue region, it will not converge to the expected operating orbit. Figure 2 (e) shows the interfaces in 3-D space for various X_0 in a cubic box. The space below the interface is the unstable region. Actually, it is clearly displayed in the slices as shown in figs. 2 (a), (b), (c) and (d). Similarly, figs. 3, 4 and 5 show the basins of attraction for different feedback parameters.

Furthermore, we observe that the yellow region diminishes as proportional coefficients K_1, K_2 increase; and vice versa. For large K_1 and K_2, the yellow region subsides and the desired operating point is almost never stable. For small K_1 and K_2, the blue region subsides and the desired operating point is almost always stable. In practice, K_1 and K_2 determine the response speed of the system. Comparing fig. 2 and fig. 3, we clearly see the limitation on selecting K_1 and K_2 so as to maintain stability for a wider basin of attraction. In addition, there are some effects for different v_{c0}. The farther it is away from the equilibrium orbit (centered around $v_{c0} = 10$V), the smaller the basin is.

Figures 4 and 5 show the basins of attraction for different integral coefficients τ_{F1} and τ_{F2}. Obviously, $1/\tau_{F1}$ and $1/\tau_{F2}$ are the zero point in the PI controller. The general trend of the variation of the basin boundaries is similar to that of Figs. 2 and 3. As $1/\tau_{F1}$ and $1/\tau_{F2}$ increase, the system goes from being globally stable to partially stable, and eventually unstable.

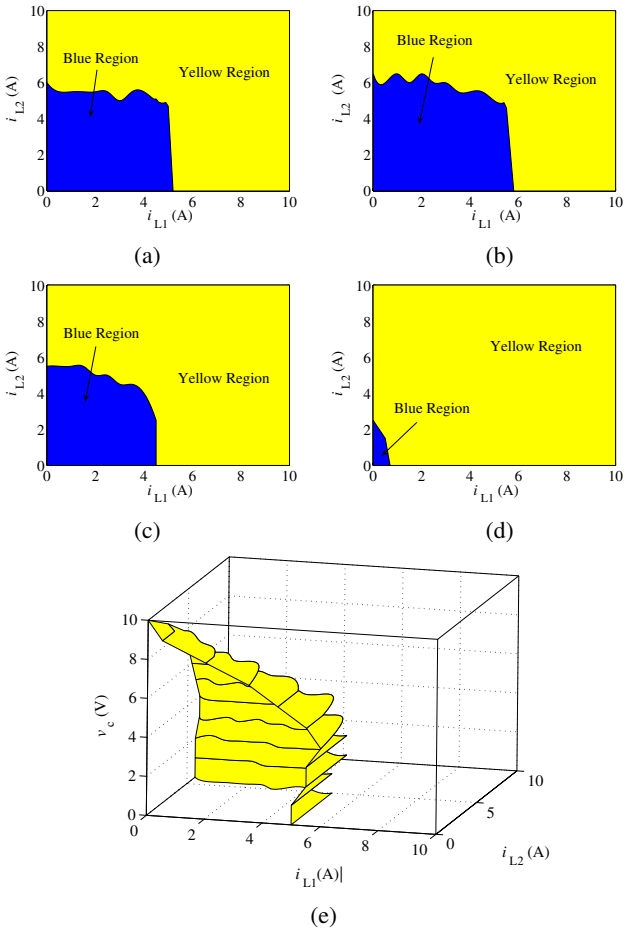

Fig. 2. Basins of attraction for $K_1 = K_2 = 5$, $1/\tau_{F1} = 1/\tau_{F2} = 12000$, $K_i = 1$. Yellow region is the basin of attraction of the desired operating orbit. Blue region is the basin of attraction of attractors other than the desired operating orbit. (a) $v_{c0} = 0$; (b) $v_{c0} = 3$; (c) $v_{c0} = 6$; (d) $v_{c0} = 9$; (e) interface in 3-D space.

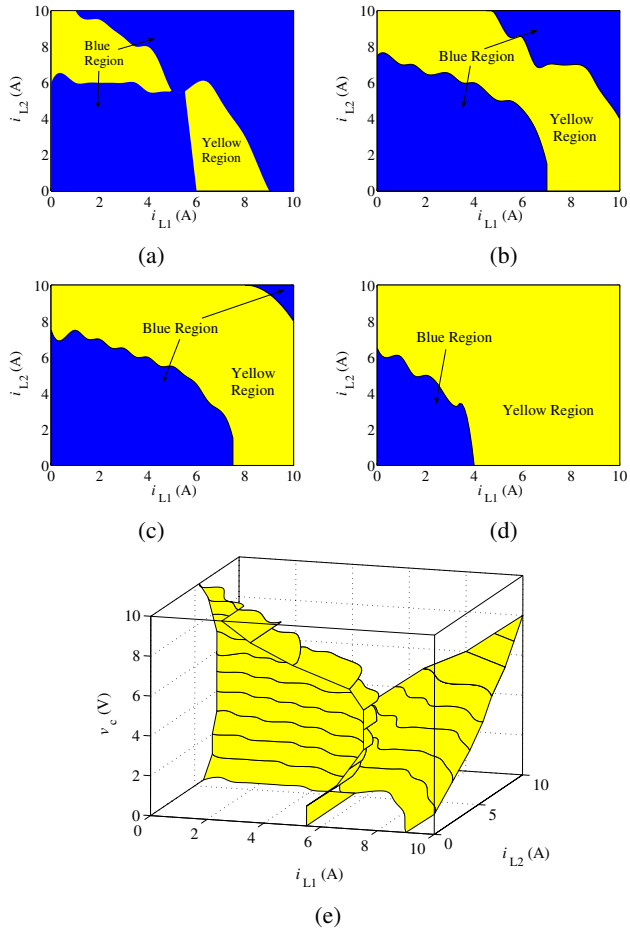

Fig. 3. Basins of attraction for $K_1 = K_2 = 6$, $1/\tau_{F1} = 1/\tau_{F2} = 12000$, $K_i = 1$. Yellow region is the basin of attraction of the desired operating orbit. Blue region is the basin of attraction of attractors other than the desired operating orbit. (a) $v_{c0} = 0$; (b) $v_{c0} = 3$; (c) $v_{c0} = 6$; (d) $v_{c0} = 9$; (e) interface in 3-D space.

Authorized licensed use limited to: Hong Kong Polytechnic University. Downloaded on December 18, 2008 at 21:51 from IEEE Xplore. Restrictions apply.

IV. Cautions on Stability Information and Stability Boundaries

From the above results, an important conclusion can be made. The stability of the operating orbit cannot be determined purely from the linear model or any method that tests stability by perturbing near the operating orbit. Stability information can be unreliable since global stability is not generally guaranteed from local stability tests. In general, we can get different stability boundaries for different initial conditions.

The stability boundaries for the parallel connected boost converter system are shown in Figs. 6, 7 and 8, corresponding to two initial points. One is the origin point $X_0 = [0,\ 0,\ 0]$, and the other is a point near the equilibrium orbit, e.g., $X_0 = [5.0,\ 5.1,\ 10]$. The curve divides the parameter space into stable region (lower) and unstable region (upper). The system works in the normal stable period-1 operation when the feedback parameters are located in the stable region. Otherwise, if the parameters crosses the boundary and enters into the unstable region, the system loses stability. In Fig. 6 (a), K_1 and K_2 decrease with $1/\tau_{F1}$, $1/\tau_{F2}$ increase. Also, the gap between the two boundaries widens as $1/\tau_{F1}$ and $1/\tau_{F2}$ increase. Within the gap, coexisting attractors exist and stability information may be unreliable. Actually, the coexisting attractors exist in single boost converters when $1/\tau_F$ is large enough, as shown in Fig. 6 (b).

Figure 7 shows the effect of the current sharing parameter K_i. Again, these two boundaries are not overlapped. Coexisting attractors exist when parameters are in the gap. In the figure, when K_i is very large, the system is easy to be unstable. Thus, the two boundaries are very close.The coexisting attractors are not obvious.

Finally, Fig. 8 shows the effects of changing the size of inductors L_1 and L_2. We fix the ratio of L_1 and L_2, and maintain the system in CCM in steady state. From the figure, we clearly observe that the coexisting attractors exist in the whole inductance range.

V. Conclusions

This paper studies the coexisting attractors in two parallel connected boost converters under master-slave current sharing

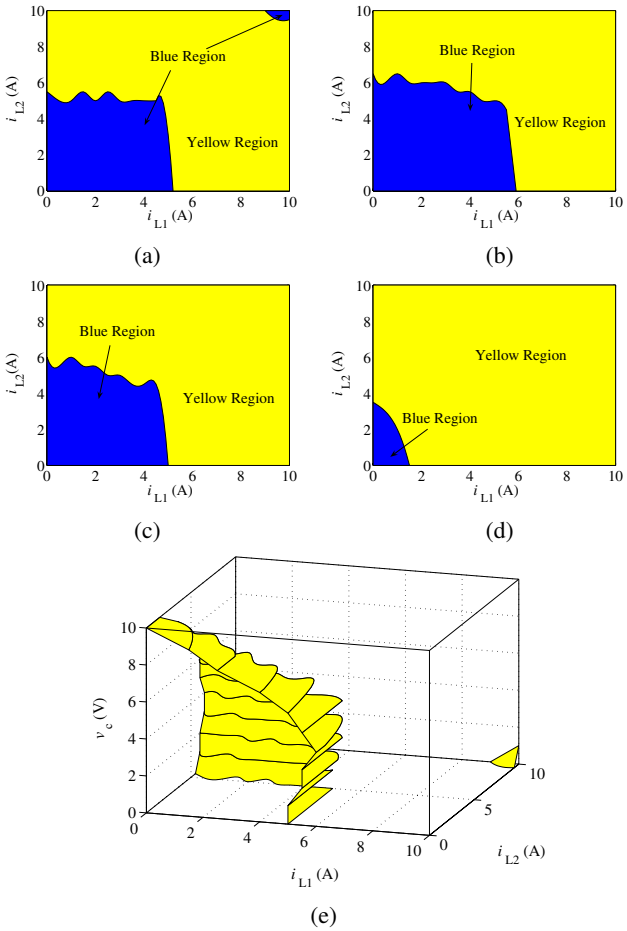

Fig. 4. Basins of attraction for $K_1 = K_2 = 5.5$, $1/\tau_{F1} = 1/\tau_{F2} = 11000$, $K_i = 1$. Yellow region is the basin of attraction of the desired operating orbit. Blue region is the basin of attraction of attractors other than the desired operating orbit. (a) $v_{c0} = 0$; (b) $v_{c0} = 3$; (c) $v_{c0} = 6$; (d) $v_{c0} = 9$; (e) interface in 3-D space.

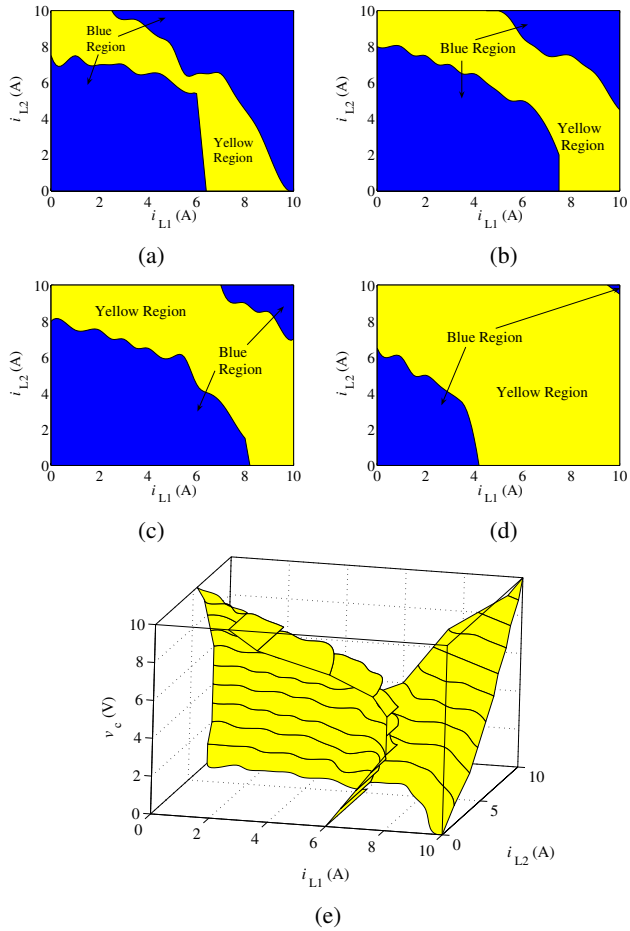

Fig. 5. Basins of attraction for $K_1 = K_2 = 5.5$, $1/\tau_{F1} = 1/\tau_{F2} = 14000$, $K_i = 1$. Yellow region is the basin of attraction of the desired operating orbit. Blue region is the basin of attraction of attractors other than the desired operating orbit. (a) $v_{c0} = 0$; (b) $v_{c0} = 3$; (c) $v_{c0} = 6$; (d) $v_{c0} = 9$; (e) interface in 3-D space.

Authorized licensed use limited to: Hong Kong Polytechnic University. Downloaded on December 18, 2008 at 21:51 from IEEE Xplore. Restrictions apply.

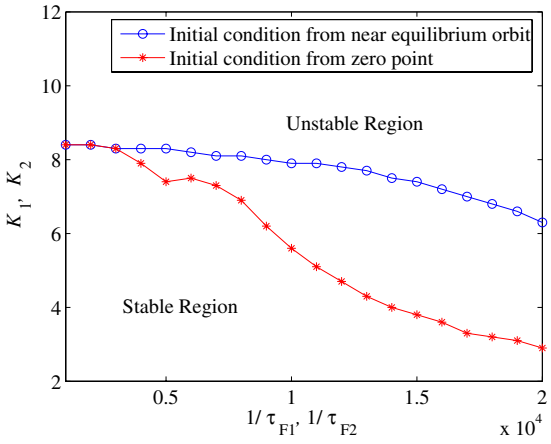

(a)

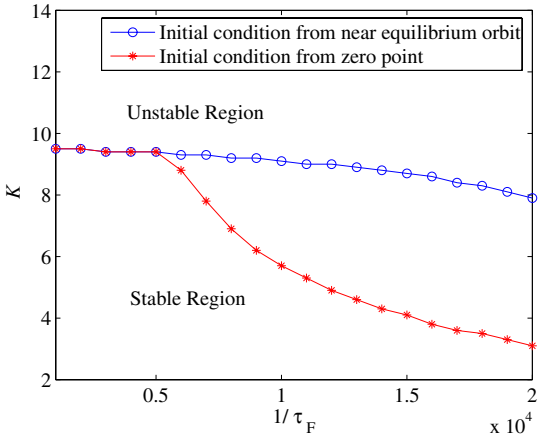

(b)

Fig. 6. Stability boundaries of feedback parameters in (a) two paralleled boost converters in $1/\tau_{F1}$, $1/\tau_{F2}$–K_1, K_2 plane for $K_i = 1$; (b) single boost converter in $1/\tau_F$–K plane.

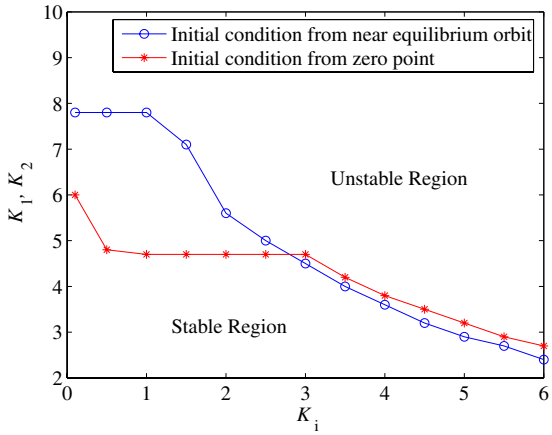

Fig. 7. Stability boundary of feedback parameters K_i versus K_1, K_2 for $1/\tau_{F1} = 1/\tau_{F2} = 12000$.

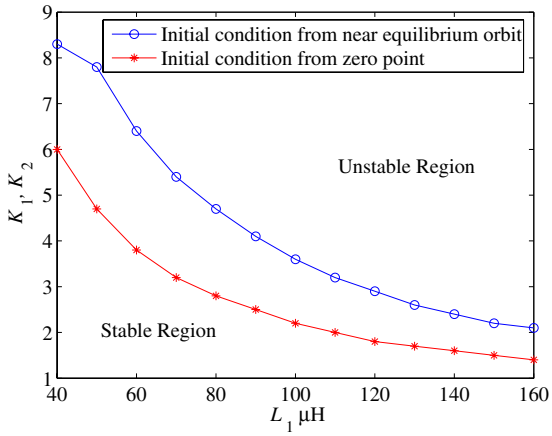

Fig. 8. Stability boundary of feedback parameters K_1, K_2 in relation to L_1 for $1/\tau_{F1} = 1/\tau_{F2} = 12000$, $K_i = 1$.

and peak-current-mode control. The system is either stable or oscillatory depending on the initial condition and the control parameters. The implication of this finding is relevant to practical operation since stability information obtained from linear models or any method that involves perturbation around the operating orbit can be unreliable. Specifically, stability information obtained from linear methods has been shown over-optimistic. Practically, enough margins have to be considered in linear methods. In fact, the basins of attraction of an operating orbit is an important piece of design information, and stability boundaries in parameter space have to be interpreted in conjunction with the initial conditions. Different initial conditions may give rise to different stability boundaries. In this paper, we have reported the phenomenon and illustrated the effects of different parameters by presenting the numerical basins of attraction and specific stability boundaries.

ACKNOWLEDGMENT

This work was supported by Hong Kong Research Grants Council under a CERG project (Ref. PolyU 5237/04E).

REFERENCES

[1] V. J. Thottuvelil and G. C. Verghese, "Analysis and control of paralleled dc/dc converters with current sharing," *IEEE Trans. Power Electron.*, vol. 13, no. 4, pp. 635–644, July 1998.

[2] J. Rajagopalan, K. Xing, Y. Guo, F. C. Lee, and B. Manners, "Modeling and dynamic analysis of paralleled DC/DC converters with master-slave current sharing control," *Proc. IEEE APEC'96*, pp. 678–684, 1996.

[3] Y. Panov, J. Rajagopalan, and F. C. Lee, "Analysis and design of N paralleled DC-DC converters with master-slave current-sharing control," *Proc. IEEE APEC'97*, pp. 436–442, 1997.

[4] K. Siri, C. Q. Lee, and T. F. Wu, "Current distribution control for parallel connected converters: Part I and Part II," *IEEE Trans. Aerospace Electron. Syst.*, vol. 28, no. 3, pp. 829–851, July 1992.

[5] C.K. Tse, *Complex Behavior of Switching Power Converters*, Boca Raton: CRC Press, 2003.

[6] Y. Huang, C. K. Tse, "On the Basins of Attraction of Parallel Connected Buck Switching Converters," *Proc. IEEE ISCAS'06*, to appear.

[7] S. Banerjee, G. C. Verghese, *Nonlinear Phenomena in Power Electronics: Attractors, Bifurcations, Chaos, and Nonlinear Control*, New York: IEEE Press, 2001.

Authorized licensed use limited to: Hong Kong Polytechnic University. Downloaded on December 18, 2008 at 21:51 from IEEE Xplore. Restrictions apply.